Exact Transfer Function Analysis of Distributed Parameter Systems by Wave Propagation Techniques

Bongsu Kang
Indiana University – Purdue University Fort Wayne
USA

1. Introduction

The vibrations of elastic structures such as strings, beams, and plates can be described in terms of waves traveling in waveguides (Cremer et al., 1973; Graff, 1975; Fahy, 1987). While the subject of wave propagation has been extensively studied in the fields of acoustics in fluids and solids rather than vibrations of elastic structures, wave analysis techniques have been employed to reveal physical characteristics associated with structural vibrations of elastic media (Argento & Scott, 1995; Kang & Tan, 1998). One of the advantages of the wave analysis technique, when applied to the structural vibration analysis, is its compact and systematic approach to analyze complex structures with discontinuities (Mace, 1984; Yong & Lin, 1989; Kang et al., 2003; Mei & Mace, 2005). Applying the concept of wave reflection and transmission, Mace (1984) obtained the frequency equations of Euler-Bernoulli beams including waves of both propagating and near-field types. By the phase-closure principle, also referred to as the wave-train closure principle (Cremer et al., 1973), Mead (1994) determined natural frequencies of Euler-Bernoulli beams. This principle states that if the phase difference between incident and reflected waves is an integer multiple of 2π, then the waves propagate at a natural frequency and their motions constitute a vibration mode. Based on the same principle, Kang (2007) presented a systematic approach to the free and forced vibration analysis of multi-span beams.

The classical method, known as the normal mode or eigenfunction expansion, of solving the forced vibration problem of a distributed parameter system involves expansion of the forcing function into the eigenfunctions of the associated free vibration problem. While this method is theoretically sound and powerful, the method is difficult to implement when the problem to be solved is a non-self-adjoint system typically due to complicating effects such as damping, discontinuities, or non-classical boundary conditions, for which case obtaining the exact eigensolutions is not often feasible. Although approximate eigensolutions may be used instead of exact ones, the problem still persists in the form of poorly convergent solution and/or significant error in the solution. As an alternative approach to solve forced vibration problems, Yang and Tan (1992) presented a method for evaluating exact closed-

form transfer functions for a class of one-dimensional distributed parameter systems. Applying the energy functionals of constrained and combined damped systems, Yang (1996a, 1996b) presented a method to obtain a closed-form transient response solution in eigenfunction series for a distributed damped system.

The dynamic displacement of any point in an elastic waveguide can be determined by superimposing the amplitudes of the constituent waves traveling along the waveguide, which is a basis of wave propagation. Based on this simple fact, an alternative technique for the free and forced vibration analysis of one-dimensional distributed parameter systems is presented. The method of normal mode expansion is often difficult to implement for nonself-adjoint systems with complicating effects such as mode couplings, non-proportional damping, discontinuities, or arbitrary boundary conditions, since the method requires eigensolutions or assumed normal modes as a priori. However, this alternative analysis technique based on the elastic wave propagation does not pose such a requirement and leads to the exact, closed-form, distributed transfer function of a distributed parameter system. The general wave solution of the equation of motion governing the dynamics of a waveguide is cast into a matrix form in terms of the constituent waves defined in the Laplace domain. The spatial amplitude variation of the traveling wave is represented by the field transfer matrix and the amplitude distortion of the traveling wave incident upon a discontinuity due to geometric or kinetic constraints is described by the local wave reflection and transmission matrices. Combining these matrices in a progressive manner along the waveguide by applying the concepts of global wave reflection and transmission matrices leads to the exact characteristic equation and corresponding mode shapes for the free response analysis and the transfer function of the system for the forced response analysis. The transient response solution for a complex system can be obtained through the Laplace inversion of the transfer function using numerical inversion algorithms. The exact frequency response solution, which includes infinite normal modes of the system, can be obtained in terms of the complex frequency response function from the transfer function. One of the main advantages of this analysis technique is its systematic formulation resulting in a recursive computational algorithm which can be implemented into highly efficient computer codes. This systematic approach also allows modular formulation which can be readily expandable to include additional discontinuities with little alteration to the existing formulation. In addition, it is also computationally advantageous that the technique always results in operating matrices of a fixed size regardless of the number of discontinuities in a waveguide. This analysis technique is applicable to any one-dimensional waveguides (strings, axial rods, torsional bars, beams, and frame structures), in particular systems with multiple point discontinuities such as viscoelastic supports, attached inertias, and geometric/material property changes. The analysis technique is demonstrated using the second order wave equation, fourth order beam equation, and sixth order curved beam equation.

2. Second order systems

The free transverse vibration of a taut string, longitudinal vibration of a thin bar, and the torsional vibration of a shaft are governed by the equation of motion in the same form, the wave equation, and thus they are mathematically analogous. Therefore, with no loss of generality, the transverse vibration of the string is taken as a representative problem for the description of the present analysis technique based on wave propagation. The equation governing the transverse motion of a uniformly damped string of span length L is

$$T\frac{\partial^2 W}{\partial X^2} + C_e \frac{\partial W}{\partial t} = m\frac{\partial^2 W}{\partial t^2} \tag{2.1}$$

where W is the transverse displacement, X the spatial variable, t the temporal variable; and T denotes the constant tension, C_e the damping coefficient, and m the mass per unit length of the string. With introduction of the following non-dimensional variables and parameters

$$w = W/L \quad x = X/L \quad \tau = t/t_0 \quad c_e = C_e L/t_0 \quad t_0 = L/c_0 \quad c_0 = \sqrt{T/m} \tag{2.2}$$

the equation of motion takes the non-dimensional form of

$$w'' + c_e \dot{w} = \ddot{w} \quad (0 \le x \le 1) \tag{2.3}$$

where the prime (') and dot (·) denote the differentiation with respect to x and τ, respectively. Applying the Laplace transform to Eq. (2.3) yields

$$\bar{w}''(x;s) + c_e s\bar{w}(x;s) = s^2\bar{w}(x;s) \tag{2.4}$$

where s denotes the Laplace variable and zero initial conditions are assumed.

2.1 Wave solution

Denoting C as the amplitude of the wave traveling along the string, the solution of Eq. (2.4) can be assumed in wave form

$$\bar{w}(x;s) = Ce^{i\gamma x} \tag{2.5}$$

where γ is the non-dimensional wavenumber normalized against span length L. Applying the above wave solution to Eq. (2.4) gives the frequency equation of the problem

$$\gamma^2 + s^2 - c_e s = 0 \text{ or } \gamma^2 = c_e s - s^2 \tag{2.6}$$

from which the general wave solution can be found as the sum of two constituent waves

$$\bar{w}(x;s) = C^+ e^{-i\gamma x} + C^- e^{i\gamma x} \tag{2.7}$$

where the coefficient C represents the amplitude of each wave component with its traveling direction indicated by the plus (+) or (−) sign. Note that γ is complex valued for nonzero c_e, hence the classification of the wave into propagating and attenuating waves does not apply to this case. Defining $f(x;s) = e^{-i\gamma x}$ as the *field transfer function* which relates the wave amplitudes by

$$C^+(x + x_0) = fC^+(x_0) \text{ or } C^-(x + x_0) = f^{-1}C^-(x_0) \tag{2.8}$$

where $f^{-1}(x;s) = e^{i\gamma x}$, the wave solution in Eq. (2.7) can be re-written as

$$\bar{w}(x;s) = fC^+ + f^{-1}C^- \tag{2.9}$$

2.2 Wave reflection and transmission

When a wave traveling along a string is incident upon a discontinuity such as an elastic support, geometric/material property change, or boundary, it is reflected and transmitted at different rates depending on the properties of the discontinuity. The rates of wave reflection and transmission can be determined in terms of *wave reflection* and *transmission coefficients*. For example, consider an infinitely long string constrained at a local coordinate $\xi = 0$ as shown in Fig. 1, where the constraint is a point support consisting of an attached mass (M_c), a transverse spring (K_c), and a viscous damper (C_c).
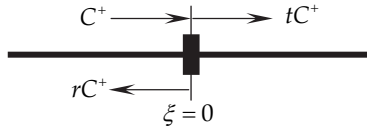

Fig. 1. Wave reflection and transmission at a discontinuity.

When a positive-traveling wave C^+ is incident upon the support, it gives rise to a reflected wave rC^+ and a transmitted wave tC^+, where r and t represent the wave reflection and transmission coefficients, respectively. The resulting transverse displacements at the left and right of the constraint are

$$\bar{w}_l = C^+ + rC^+ \quad \bar{w}_r = tC^+ \tag{2.10}$$

Since $\bar{w}_l = \bar{w}_r$ at ξ=0, one can find

$$1 + r = t \tag{2.11}$$

In addition, the kinetic equilibrium condition at ξ=0 states that

$$\bar{w}'_r - \bar{w}'_l = \varphi\bar{w}_r \tag{2.12}$$

where φ represents the kinetic properties of the constraint as

$$\varphi(s) = k_c + c_c s + m_c s^2 \tag{2.13}$$

Note that k_c, c_c, and m_c in Eq. (2.13) are the non-dimensional spring constant, damping coefficient, and the attached mass, respectively, defined by

$$k_c = K_c L/T \quad c_c = C_c c_0/T \quad m_c = M_c c_0^2/TL \tag{2.14}$$

Equation (2.12) leads to

$$\gamma(r + t - 1) = i\varphi t \tag{2.15}$$

Combining Eqs. (2.11) and (2.15), the wave reflection and transmission coefficients can be found as

$$r = \frac{i\varphi}{2\gamma - i\varphi} \quad \text{and} \quad t = \frac{2\gamma}{2\gamma - i\varphi} \tag{2.16}$$

When a wave is incident upon a boundary at $\xi=0$, it is only reflected, therefore

$$\overline{w}'_l = -\varphi\overline{w}_l \tag{2.17}$$

which leads to

$$r = \frac{\gamma + i\varphi}{\gamma - i\varphi} \tag{2.18}$$

In the limiting case where $\varphi=\infty$, it can be seen that $r=-1$ which is the wave reflection coefficient for the classical fixed boundary. When the wave is incident upon a series of discontinuities along its traveling path, it is more computationally efficient to employ the concepts of *global wave reflection and transmission coefficients*, in particular when the free or forced vibration analysis of a multi-span string is sought. These coefficients relate the amplitudes of incoming and outgoing waves at a discontinuity. Consider wave motion in a multi-span string as illustrated in Fig. 2. Define R_{ir} as the global wave reflection coefficient which relates the amplitudes of negative- and positive-traveling waves on the right side of discontinuity i such that

$$C_{ir}^- = R_{ir}C_{ir}^+ \tag{2.19}$$

Fig. 2. Waves traveling along a multi-span string.

Since $C_{ir}^- = f_i R_{(i+1)l} C_{ir}^+$, one can find R_{ir} in terms of the global wave reflection coefficient on the left side of discontinuity $i+1$; i.e.,

$$R_{ir} = f_i^2 R_{(i+1)l} \tag{2.20}$$

In addition, by combining the following wave equations at discontinuity i

$$C_{ir}^+ = t_i C_{il}^+ + r_i C_{ir}^- \text{ and } C_{il}^- = t_i C_{ir}^- + r_i C_{il}^+ \tag{2.21-22}$$

the relationship between the global wave reflection coefficients on the left and right sides of discontinuity i can be found as

$$R_{il} = r_i + t_i^2 (R_{ir}^{-1} - r_i)^{-1} \tag{2.23}$$

R_{ir} and R_{il} progressively expand to include all the global wave reflection coefficients of discontinuities along the string before terminating its expansion at the boundaries where

$$C_1^+ = r_1 C_1^- \quad C_n^- = r_n C_n^+ \tag{2.24}$$

While the global wave reflection coefficient relates the amplitudes of waves traveling in the opposite direction of each other within a subspan i, there is a need for another coefficient which relates the amplitudes of waves traveling in the same direction in two adjacent subspans. This inter-span coefficient is particularly useful when the mode shape or forced response of a string with several or more subspans needs to be determined since it allows an intuitive and systematic formulation of the system's transfer function. Denoting this inter-span wave transfer coefficient as the *global wave transmission coefficient T_i*, define

$$C_{ir}^+ = T_i C_{(i-1)r}^+ \tag{2.25}$$

Rewriting Eq. (2.21) by applying $C_{il}^+ = f_{(i-1)} C_{(i-1)r}^+$ and $C_{ir}^- = R_{ir} C_{ir}^+$, and then comparing it with Eq. (2.25), the global wave transmission coefficient at discontinuity i can be found as

$$T_i = (1 - r_i R_{ir})^{-1} t_i f_{(i-1)} \tag{2.26}$$

The global wave reflection and transmission coefficients are the key elements in determining the exact transfer function of a multi-span string as discussed in the following sections.

2.3 Free response analysis

The global reflection and transmission coefficients of waves traveling along a multi-span sting are now combined with the field transfer function to analyze the free response of a multi-span sting. With reference to Fig. 2, consider wave motion in the first span. Based on the definition of the global wave reflection coefficient, at the boundary

$$C_1^- = R_{1r} C_1^+ \tag{2.27}$$

However, recalling $C_1^+ = r_1 C_1^-$ from Eq. (2.24), it can be found that

$$(r_1 R_{1r} - 1) C_1^+ = 0 \tag{2.28}$$

For nontrivial solutions,

$$F(s) = r_1 R_{1r} - 1 = 0 \tag{2.29}$$

which is the characteristic equation in terms of the Laplace variable s for the multi-span string with arbitrary discontinuities and boundaries. This remarkably simple expression for the characteristic equation is due to the fact that R_{1r} recursively expands to include all the effects of constraints in the remaining side of the string until its expansion terminates at the rightmost boundary which yields $R_{nl}=r_n$. This equation simply states that when the string system vibrates at one of its natural frequencies, $r_1 R_{1r}=1$. As a simple example, for a single span uniformly damped string fixed at both ends, $r_1=r_2=-1$ from Eq. (2.18) and $R_{1r}=e^{-2i\gamma}$ from Eq. (2.20). Therefore, $F(s)=e^{-2i\gamma}-1=0$ gives the natural wavenumbers $\gamma_n=n\pi$ ($n=1,2,3,...$), or in terms of the non-dimensional frequency $\omega_n^2 + i c_e \omega_n = (n\pi)^2$ by Eq. (2.6) with s replaced by $i\omega$.

The mode shapes of the multi-span string system can be found in a systematic manner by relating wave amplitudes between two adjacent subspans. Let ξ_i denote the local coordinate within span i. The transverse displacement at any point in span i can be expressed as

$$\overline{w}_i(\xi_i) = f_i(\xi_i)C_i^+ + f_i^{-1}(\xi_i)C_i^- \tag{2.30}$$

However, due to Eq. (2.19)

$$\overline{w}_i(\xi_i) = [f_i(\xi_i) + f_i^{-1}(\xi_i)R_{ir}]C_i^+ \tag{2.31}$$

Now by applying the global wave transmission coefficient defined in Eq. (2.25) to C_i^+ in the above equation, the displacement at any point in span i of the string can be expressed in terms of the wave amplitude in span i–1 as

$$\overline{w}_i(\xi_i) = [f_i(\xi_i) + f_i^{-1}(\xi_i)R_{ir}]T_iC_{i-1}^+ \tag{2.32}$$

Assume a disturbance arise in span 1; i.e., a wave originates and starts traveling from the leftmost boundary of the string. Then, by successively applying the global transmission coefficient of each discontinuity on the way up to the first span, the mode shape of span i can be found in terms of wave amplitude C_1^+; i.e.,

$$\overline{w}_i(\xi_i) = [f_i(\xi_i) + f_i^{-1}(\xi_i)R_{ir}]\prod_{j=i}^{1}T_jC_1^+ \quad C_1^+ \quad 0 \le \xi_i \le l_i \tag{2.33}$$
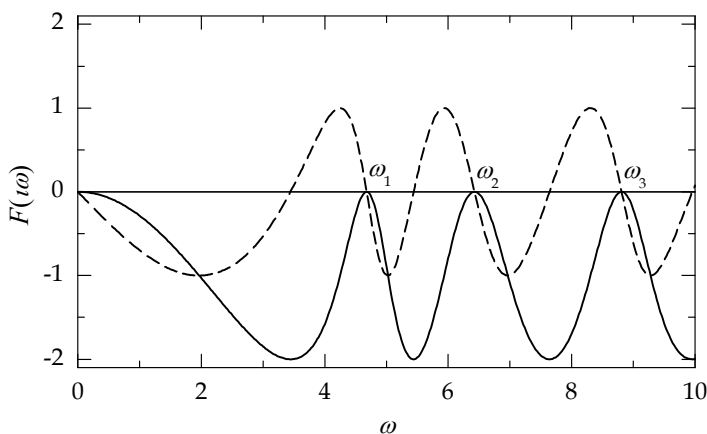
Fig. 3. Plot of the characteristic equation. The solid and dashed curves represent the real and imaginary parts, respectively.

For example, consider a fixed-fixed undamped string with three supports specified by $\varphi_2=5+0.1s^2$, $\varphi_3=7+0.1s^2$, and $\varphi_4=4+0.1s^2$ according to Eq. (2.13). $l_1=0.25$, $l_2=0.3$, $l_3=0.25$, and $l_4=0.2$ are assumed. Once the global wave reflection coefficient at each discontinuity has been determined, one can apply Eq. (2.29) to find the natural frequencies. Shown in Fig. 3 is the plot of the characteristic equation, where the first three natural frequencies are indicated. The mode shapes can be found from Eq. (2.33) in a systematic way once the global wave transmission coefficient at each discontinuity has been determined. Figure 4 shows the mode shapes for the first three modes.
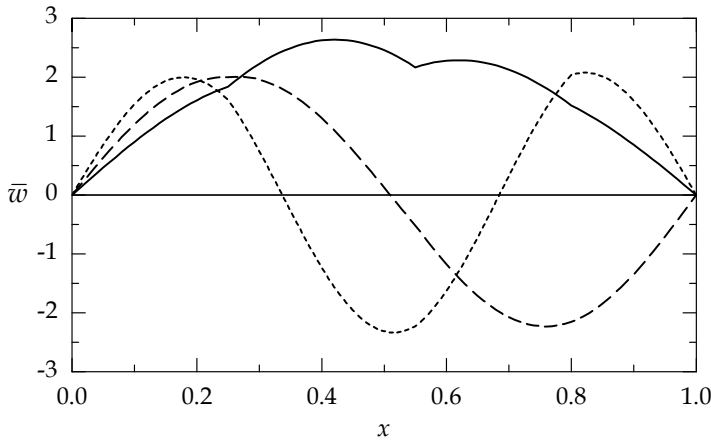
Fig. 4. First three mode shapes obtained from Eq. (2.33). The solid, dashed, and dotted curves represent the 1st , 2nd, and 3rd modes, respectively.

2.4 Transfer function analysis

Consider a multi-span string subjected to an external point load $\bar{p}(s)$, normalized against tension T, applied at $x=x_0$ as shown in Fig. 5. Since the waves injected by the load travel in both direction from the point of loading, a set of local coordinates $\{\xi, \xi^*\}$ is introduced such that the wave traveling toward each boundary of the string is considered positive as indicated in Fig. 5. Let $C_1^{\pm}$ and $D_1^{\pm}$ denote the injected waves that travel in the region $x<x_0$ and $x \geq x_0$ within span 1, respectively. The transverse displacement of span 1 of the string can be expressed as
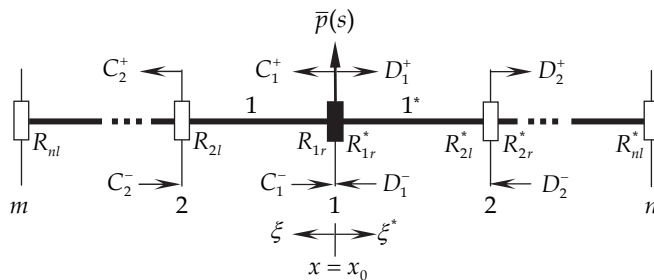
Fig. 5. Wave motion in a multi-span string due to a point load.

$$\bar{w}_1(\xi_1, x_0; s) = f_1(\xi_1; s)C_1^+ + f_1^{-1}(\xi_1; s)C_1^- \quad 0 \leq \xi_1 \leq l_1 \tag{2.34}$$

Defining v as the wave injected by the applied load, the difference in amplitudes between the incoming and outgoing waves at the loading point is

$$C_1^+ - D_1^- = v \quad D_1^+ - C_1^- = v \tag{2.35}$$

where v can be determined from the geometric and kinetic continuity conditions at $\xi=0$ as

$$v = \frac{\sqrt{-1}}{2\gamma}\overline{p}(s) \tag{2.36}$$

Applying the global wave reflection coefficient on each side of the loading point gives

$$C_1^- = R_{1r}C_1^+ \quad D_1^- = R_{1r}^*D_1^+ \tag{2.37}$$

where the asterisk (*) signifies that the global wave reflection coefficient is defined in the region $x \geq x_0$ to distinguish it from the one defined in the region $x < x_0$. Combining Eqs. (2.35) and (37), one can determine the ampltitude of the wave that rises at the loading point in each direction

$$C_1^+ = T_1 v \quad T_1 = (1 - R_{1r}^* R_{1r})(1 + R_{1r}^*) \tag{2.38.1}$$

$$D_1^+ = T_1^* v \quad T_1^* = (1 - R_{1r} R_{1r}^*)(1 + R_{1r}) \tag{2.38.2}$$

Note that T_1 and T_1^* and can be considered as the global wave transmission coefficients that characterize the transmissibility of the wave injected by the external force in the region $x < x_0$ and $x \geq x_0$, respectively. It is evident that and T_1 and T_1^* are different unless the string system is symmetric about the loading point. Applying the results in Eqs. (2.37) and (2.38) to Eq. (2.34), the wave motion in either side of $x = x_0$ can be found; i.e., in the region $x < x_0$

$$\overline{w}_1(\xi_1, x_0; s) = [f_1(\xi_1; s) + f_1^{-1}(\xi_1; s)R_{1r}]T_1 v \quad 0 \leq \xi_1 \leq l_1 \tag{2.39}$$

Now, in the same manner as for the mode shape analysis, since $C_{i+1}^+ = T_i C_i^+$ and $C_1^+ = T_1 v$, the wave motion in span i on either side of the loading point can be found. For the region $x < x_0$

$$\overline{w}_i(\xi_i, x_0; s) = [f_i(\xi_i; s) + f_i^{-1}(\xi_i; s)R_{ir}]\prod_{k=i}^{1} T_k v \quad 0 \leq \xi_i \leq l_i \tag{2.40}$$

Note that the ratio

$$G_i(\xi_i, x_0; s) = \overline{w}_i(\xi_i, x_0; s)/\overline{p}(s) \tag{2.41}$$

is the transfer function governing the forced response of any point in span i due to the point loading at $x = x_0$. The Laplace inversion of $G_i(\xi_i, x_0; s)$ is the Green's function of the problem. Thefore, denoting L^{-1} as the inverse Laplace transform operator, the forced response at any point within any subspan of the multi-span string can be determined from the following convolution integral; e.g., for span i in the region $x < x_0$

$$w_i(\xi_i, x_0; \tau) = \int_0^\tau G_i(\xi_i, x_0; \tau - \overline{\tau})p(\tau)d\overline{\tau} \quad (i = 1, 2, \cdots, m) \tag{2.42.1}$$

$$G_i(\xi_i, x_0; \tau) = L^{-1}[\frac{\sqrt{-1}}{2\gamma}[f_i(\xi_i; s) + f_i^{-1}(\xi_i; s)R_{ir}]\prod_{k=i}^{1} T_1] \quad 0 \leq \xi_i \leq l_i \tag{2.42.2}$$

The exact Laplace inversion of $G_i(\xi_i, x_0; s)$ in close form is not feasible in general, in particular for multi-span string systems. One may have to resort to the numerical inversion of Laplace transforms. It is found that the algorithm known as the fixed Talbot method (Abate & Valko, 2004), which is based on the contour of the Bromwich inversion integral, appears to perform the numerical Laplace inversion in Eq. (2.42) with a satisfactory accuracy and reasonable computation time. In this method, the accuracy of the results depends only on the number of precision decimal digits (denoted with M in the algorithm) carried out during the inversion. It is found that for well-damped second- and higher order distributed parameter systems, $M=32$ and for lightly damped or undamped systems, $M=64$ gives acceptable results. To demonstrate the effectiveness of the present analysis approach, consider the unit impulse response of a single span undamped string, in particular the response near the point of loading immediately after the loading, which is well known for its deficiency in numerical convergence. The response solution by the method of normal mode expansion is

$$w(x, x_0; \tau) = \sum_{n=1}^{N} \frac{2 \sin n\pi x_0}{n\pi} \sin n\pi x \sin n\pi\tau \qquad (2.43)$$

The corresponding transfer function from Eq. (2.40) is

$$\bar{w}(x, x_0; s) = \frac{1}{2s(e^{2s} - 1)} \begin{cases} e^{-sx}(e^{2s(1-x_0)} - 1)(e^{2sx} - e^{2sx_0}) & \text{for } 0 \le x \le x_0 \\ e^{-sx}(e^{2sx_0} - 1)(e^{2sx} + e^{2s(1-x_0)}) & \text{for } x_0 < x \le 1 \end{cases} \qquad (2.44)$$
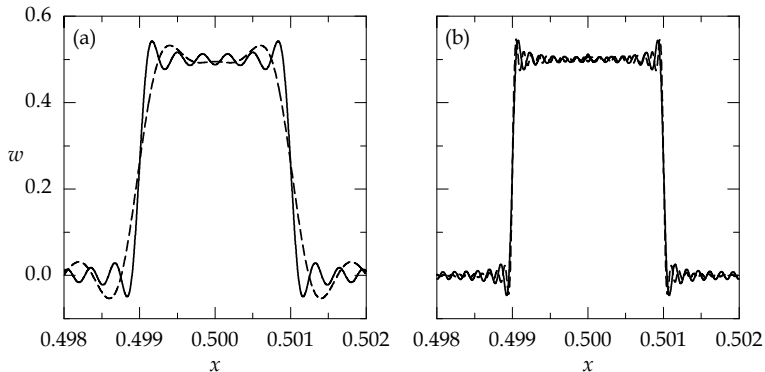

Fig. 6. Unit impulse response of a single span string near the point of loading at $\tau=0.001$: (a) $M=32$ and $N=2,500$; (b) $M=64$ and $N=20,000$. The solid and dashed curves represent the solutions from Eqs. (2.43) and (2.44), respectively.

Shown in Fig. 6 is the comparison of the response solutions given in Eqs. (2.43) and (2.44) when $\tau=0.001$ near $x=x_0=0.5$. $N=2,500$ and $N=20,000$ are used for the evaluation of the series solution, while $M=32$ and $M=64$ are used for the numerical Laplace inversion of the transfer function in Eq. (2.44). It can be seen that the series solution in Eq. (2.43) fails to accurately represent the actual impulse response behavior with $N=2,500$. This is expected for the series solution since it would take a large number of harmonic terms ($N \ge 10,000$ for this example)

to represent such a sharp spike due to the impulse. It can be seen that the result with $M{=}32$ reasonably represents the actual behavior, and the result with $M{=}64$ is almost comparable to the series solution with $N{=}20,000$. However, if one tries to obtain the response at a time very close to the moment of impact, the numerical Laplace inversion becomes extremely strenuous or beyond the machine precision of the computing machine. This is because the expected response would consist of waves that have unrealistically short wavelengths. This is not a unique problem for the present wave approach since the same problem would manifest itself in the series solution given in Eq. (2.43), requiring an impractically large number of harmonics terms for a convergent solution.

If $p(\tau) = p_0 e^{i\omega\tau}$; i.e., a harmonic forcing function, the steady-state response of the problem can be readily found in terms of the complex frequency function defined as

$$H(\xi_i, x_0; \omega) = G(\xi_i, x_0; s)|_{s=i\omega} \tag{2.45}$$

Therefore the frequency response at any point within any subspan of the string can be obtained by; e.g., for span i in the region $x{<}x_0$

$$w_i(\xi_i, x_0; \tau) = |H_i(\xi_i, x_0; \omega)| \, p_0 e^{i(\omega\tau + \phi_i)} \quad 0 \le \xi_i \le l_i \tag{2.46.1}$$

$$H_i(\xi_i, x_0; \omega) = \frac{\sqrt{-1}}{2\gamma}[f_i(\xi_i; \omega) + f_i^{-1}(\xi_i; \omega)R_{ir}] \prod_{k=i}^{1} T_k \quad \phi_i = \angle H_i \tag{2.46.2}$$

One of the main advantages of this approach is its systematic formulation resulting in a recursive computational algorithm which can be implemented into highly efficient computer codes consuming less computer resources. This systematic approach also allows modular formulation which can be easily expandable to include additional subspans with very minor alteration to the existing formulation. Another significant advantage of the present wave-based approach to the forced response analysis of a multi-span string is that the eigensolutions of the system is not required as a priori as in the method of normal mode expansion which assumes the forced response solution in terms of an infinite series of the system eigenfunctions – truncated later for numerical computations. However, exact eigensolutions are often difficult to obtain particularly for non-self-adjoint systems, and also approximated eigensolutions can result in large error. In contrast, the current analysis technique renders closed-form transfer functions from which exact frequency response solutions can be obtained.

3. Fourth order systems

The analysis techniques described by using the vibration of a string can be applied to the transverse vibration of a beam of which equation of motion is typically a fourth order partial differential equation. Denoting X and t as the spatial and temporal variables, respectively, the equation of motion governing the transverse displacement $W(X,t)$ of a damped uniform Euler-Bernoulli beam of length L subjected to an external load $P(X,t)$ is

$$m\frac{\partial^2 W}{\partial t^2} + C_e \frac{\partial W}{\partial t} + EI\frac{\partial^4 W}{\partial X^4} = P(X,t) \tag{3.1}$$

where m denotes the mass per unit length, EI the flexural rigidity, C_e the external damping coefficient of the beam. With introduction of the following non-dimensional variables and parameters

$$w = W/L, \ x = X/L, \ \tau = t/t_0, \ t_0 = mL^4/EI \ \ c_e = C_e t_0/m, \ p(x,t) = P(X,t)L^3/EI \quad (3.2)$$

the equation of motion takes the non-dimensional form of

$$\ddot{w} + c_e \dot{w} + w^{(4)} = p(x,t) \quad (0 \leq x \leq 1) \quad (3.3)$$

Applying the Laplace transform to Eq. (3.3) yields

$$s^2 \overline{w}(x;s) + c_e s \overline{w}(x;s) + \overline{w}^{(4)}(s;x) = \overline{p}(x;s) \quad (3.4)$$

Letting $\overline{p}(x;s) = 0$, the homogeneous wave solution of Eq. (3.4) can be assumed as:

$$\overline{w}(x;s) = C e^{i\gamma x} \quad (3.5)$$

where γ is the non-dimensional wavenumber normalized against span length L. Applying the above wave solution to Eq. (3.4) gives the frequency equation of the problem

$$\gamma^4 = -(s^2 + c_e s) \quad (3.6)$$

from which the general wave solution can be found as the sum of four constituent waves

$$\overline{w}(x;s) = C_a^+ e^{-i\gamma x} + C_a^- e^{i\gamma x} + C_b^+ e^{-\gamma x} + C_b^- e^{\gamma x} \quad (3.7)$$

where the coefficient C represents the amplitude of each wave with its traveling direction indicated by the superscript; plus (+) and minus (–) signs denote the wave's traveling directions with respect to the x-coordinate. The subscripts a and b signify the spatial wave motion of the same type traveling in the opposite direction. Note that γ is complex valued in general. The general wave solution in Eq. (3.7) may be re-expressed in vector form by grouping the wave components (wave packet) traveling in the same direction; i.e.,

$$\mathbf{C}^+ = \begin{Bmatrix} C_a^+ \\ C_b^+ \end{Bmatrix} \quad \mathbf{C}^- = \begin{Bmatrix} C_a^- \\ C_b^- \end{Bmatrix} \quad (3.8)$$

and then

$$\overline{w}(x;s) = [1 \quad 1][\mathbf{f}(x;s)\mathbf{C}^+ + \mathbf{f}^{-1}(x;s)\mathbf{C}^-] \quad (3.9)$$

where $\mathbf{f}(x;s)$ is the diagonal *field transfer matrix* (Mace, 1984) given by

$$\mathbf{f}(x;s) = \begin{bmatrix} e^{-i\gamma x} & 0 \\ 0 & e^{-\gamma x} \end{bmatrix} \quad (3.10)$$

which relates the wave amplitudes by

$$\mathbf{C}^+(x + x_0) = \mathbf{f}\mathbf{C}^+(x_0) \ \text{ or } \ \mathbf{C}^-(x + x_0) = \mathbf{f}^{-1}\mathbf{C}^-(x_0) \quad (3.11)$$

3.2 Wave reflection and transmission matrices

For a wave packet with multiple wave components, the rates of wave reflection and transmission at a point discontinuity can be found in terms of the *wave reflection matrix* **r** and *wave transmission matrix* **t**, in the same manner described in Section 2.2. When the flexural wave packet in Eq. (3.8) travels along a beam and is incident upon a kinetic constraint (ξ=0) which consists of, for example, transverse (K_t) and rotational (K_r) springs and transverse damper (C_t), **r** and **t** at the discontinuity can be found by applying the geometric continuity kinetic equilibrium conditions at ξ=0; i.e., with reference to Fig. 7, one can establish the following matrix equations

$$\begin{bmatrix} 1 & 1 \\ -i & -1 \end{bmatrix}\mathbf{C}^+ + \begin{bmatrix} 1 & 1 \\ i & 1 \end{bmatrix}\mathbf{r}\mathbf{C}^+ = \begin{bmatrix} 1 & 1 \\ -i & -1 \end{bmatrix}\mathbf{t}\mathbf{C}^+ \tag{3.12.1}$$

$$\begin{bmatrix} 1 & -1 \\ i & -1 \end{bmatrix}\mathbf{C}^+ + \begin{bmatrix} 1 & -1 \\ -i & 1 \end{bmatrix}\mathbf{r}\mathbf{C}^+ = \begin{bmatrix} 1-ik_r/\gamma & -1-k_r/\gamma \\ i+(k_t+c_ts)/\gamma^3 & -1+(k_t+c_ts)/\gamma^3 \end{bmatrix}\mathbf{t}\mathbf{C}^+ \tag{3.12.2}$$

where $k_t = K_t L^3/EI$, $k_r = K_r L/EI$, and $c_t = C_t t_0/m$. Solving the above equations gives the local wave reflection and transmission matrices as:

$$\mathbf{r} = \frac{1}{2}\begin{bmatrix} (1-i)(\alpha-\beta i) & -(1+i)(\alpha+\beta) \\ -(1-i)(\alpha+\beta) & (1+i)(\alpha+\beta i) \end{bmatrix} \tag{3.13.1}$$

$$\mathbf{t} = \frac{1}{2}\begin{bmatrix} 2-(1-i)\alpha-(1+i)\beta & (1+i)(\alpha-\beta) \\ (1-i)(\alpha-\beta) & 2-(1+i)\alpha-(1-i)\beta \end{bmatrix} \tag{3.13.2}$$

$$\alpha = \frac{k_r+c_rs}{k_r+c_rs+(2+2i)\gamma} \quad \beta = \frac{k_t+c_ts}{k_t+c_ts-(2-2i)\gamma^3}$$
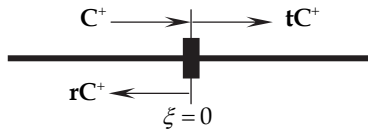
Fig. 7. Wave reflection and transmission at a discontinuity.

However, as previously discussed in Section 2.2, when the wave packet is incident upon a series of discontinuities along its traveling path, it is more computationally efficient to employ the concepts of *global wave reflection* and *transmission matrices*. These matrices relate the amplitudes of incoming and outgoing waves at a point discontinuity. When compared to the string problem, the only difference in formulating these matrices for the beam problem is to use vectors and matrices instead of single coefficients. Therefore, with reference to Fig. 2, let $\mathbf{R}_{ir}$ as the global wave reflection matrix which relates the amplitudes of negative- and positive-traveling waves on the right side of discontinuity i such that

$$\mathbf{C}_{ir}^- = \mathbf{R}_{ir}\mathbf{C}_{ir}^+ \tag{3.14}$$

Since $\mathbf{C}_{ir}^{-} = \mathbf{f}_i \mathbf{R}_{(i+1)l} \mathbf{C}_{ir}^{+}$, one can find $\mathbf{R}_{ir}$ in terms of the global wave reflection matrix on the left side of discontinuity $i+1$; i.e.,

$$\mathbf{R}_{ir} = \mathbf{f}_i \mathbf{R}_{(i+1)l} \mathbf{f}_i \qquad (3.15)$$

In addition, by combining the following wave equations at discontinuity i

$$\mathbf{C}_{ir}^{+} = \mathbf{t}_i \mathbf{C}_{il}^{+} + \mathbf{r}_i \mathbf{C}_{ir}^{-} \quad \mathbf{C}_{il}^{-} = \mathbf{t}_i \mathbf{C}_{ir}^{-} + \mathbf{r}_i \mathbf{C}_{il}^{+} \qquad (3.16\text{-}17)$$

the relationship between the global wave reflection matrices on the left and right sides of discontinuity i can be found as

$$\mathbf{R}_{il} = \mathbf{r}_i + \mathbf{t}_i (\mathbf{R}_{ir}^{-1} - \mathbf{r}_i)^{-1} \mathbf{t}_i \qquad (3.18)$$

$\mathbf{R}_{ir}$ and $\mathbf{R}_{il}$ progressively expand to include all the global wave reflection matrices of intermediate discontinuities along the beam before terminating its expansion at the boundaries. Since incident waves are only reflected at the boundaries, one can find the following wave equations

$$\mathbf{C}_1^{+} = \mathbf{r}_1 \mathbf{C}_1^{-} \quad \mathbf{C}_n^{-} = \mathbf{r}_n \mathbf{C}_n^{+} \qquad (3.19.1\text{-}2)$$

where $\mathbf{r}$ can be found by imposing the force and moment equilibrium conditions at the boundary; e.g., for the same kinetic constraint previously considered

$$\mathbf{r} = \begin{bmatrix} \gamma - ik_r & -\gamma - k_r \\ -i\gamma^3 - (k_t + c_t s) & \gamma^3 - (k_t + c_t s) \end{bmatrix}^{-1} \begin{bmatrix} \gamma + ik_r & -\gamma + k_r \\ i\gamma^3 - (k_t + c_t s) & -\gamma^3 - (k_t + c_t s) \end{bmatrix} \qquad (3.20)$$

Now, to determine the global wave transmission matrix $\mathbf{T}_i$, define

$$\mathbf{C}_{ir}^{+} = \mathbf{T}_i \mathbf{C}_{(i-1)r}^{+} \qquad (3.21)$$

Rewriting Eq. (3.16) by applying $\mathbf{C}_{il}^{+} = \mathbf{f}_{(i-1)} \mathbf{C}_{(i-1)r}^{+}$ and $\mathbf{C}_{ir}^{-} = \mathbf{R}_{ir} \mathbf{C}_{ir}^{+}$, and then comparing it with Eq. (3.21), one can find that

$$\mathbf{T}_i = (\mathbf{I}_{2\times2} - \mathbf{r}_i \mathbf{R}_{ir})^{-1} \mathbf{t}_i \mathbf{f}_{(i-1)} \qquad (3.22)$$

where $\mathbf{I}_{2\times2}$ is the 2×2 identity matrix.

3.3 Free response analysis

The global reflection and transmission matrices of waves traveling along a multi-span beam are now combined with the field transfer matrix to analyze the free vibration of the beam. With reference to Fig. 2, where $C_i^{\pm}$, R_i, and f_i are now replaced by $\mathbf{C}_i^{\pm}$, $\mathbf{R}_i$, and $\mathbf{f}_i$, respectively, at the left boundary

$$\mathbf{C}_1^{-} = \mathbf{R}_{1r} \mathbf{C}_1^{+} \qquad (3.23)$$

However, due to Eq. (3.19), it can be found that

$$(\mathbf{r}_1\mathbf{R}_{1r} - \mathbf{I}_{2\times 2})\mathbf{C}_1^+ = \mathbf{0} \tag{3.24}$$

Applying the condition for non-trivial solutions to the above matrix equation, one can obtain the following characteristic equation in terms of the Laplace variable s

$$F(s) = \mathrm{Det}[\mathbf{r}_1\mathbf{R}_{1r} - \mathbf{I}_{2\times 2}] = 0 \tag{3.25}$$

By applying a standard root search technique (e.g., Newton-Raphson method or secant method) to Eq. (3.25), one can obtain the natural frequencies of the multi-span beam.

The mode shapes of the multi-span beam can be systematically found by relating wave amplitudes between two adjacent subspans, in the same way described in Section 2.3. Defining ξ_i as the local coordinate in span i, the transverse displacement of any point in span i can be found as

$$\bar{w}_i(\xi_i) = [1 \quad 1][\mathbf{f}_i(\xi_i)\mathbf{C}_i^+ + \mathbf{f}_i^{-1}(\xi_i)\mathbf{C}_i^-] \tag{3.26}$$

However, due to Eq. (3.14)

$$\bar{w}_i(\xi_i) = [1 \quad 1][\mathbf{f}_i(\xi_i) + \mathbf{f}_i^{-1}(\xi_i)\mathbf{R}_{ir}]\mathbf{C}_i^+ \tag{3.27}$$

Since $\mathbf{C}_i^+ = \mathbf{T}_i\mathbf{C}_{i-1}^+$ from Eq. (3.21),

$$\bar{w}_i(\xi_i) = [1 \quad 1][\mathbf{f}_i(\xi_i) + \mathbf{f}_i^{-1}(\xi_i)\mathbf{R}_{ir}]\mathbf{T}_i\mathbf{C}_{i-1}^+ \tag{3.28}$$

Assume a wave packet originates and starts traveling from the leftmost boundary of the beam. By successively applying the global transmission matrix of each discontinuity on the way up to the first span, the mode shape of span i can be found in terms of wave amplitude $\mathbf{C}_1^+$; i.e.,

$$\bar{w}_i(\xi_i) = [1 \quad 1][\mathbf{f}_i(\xi_i) + \mathbf{f}_i^{-1}(\xi_i)\mathbf{R}_{ir}]\prod_{j=i}^{1}\mathbf{T}_j\mathbf{C}_1^+ \quad \mathbf{T}_1 = \mathbf{I}_{2\times 2} \quad 0 \le \xi_i \le l_i \tag{3.29}$$

Constraint	Discontinuity					
	1	2	3	4	5	6
Location	0	0.15	0.35	0.6	0.82	1
k_t	∞	3,000	2,500	1,500	3,500	∞
k_r	0	250	150	100	300	∞
c_t	0	0	0	0	0	0

Table 1. Nondimensional system parameter used for Fig. 8.

where note that the amplitude ratio between the two wave components C_a^+ and C_b^+ can be found from Eq. (3.24). For example, shown in Fig. 8 are the first three mode shapes of a uniformly damped five-span beam with system parameters specified in Table 1. Once the wave reflection and transmission matrices at each discontinuity and the boundary are determined, one can apply Eq. (3.25) to find the first three natural wavenumbers $\gamma_1 = 10.294$, $\gamma_2 = 12.038$, and $\gamma_3 = 14.148$, from which the damped natural frequencies of the beam can be determined by using Eq. (3.6). It should be noted from the computational point of view that

the present wave approach always results in operationg matrices of a fixed size regardless of the number of subspans. However if the classical method of separation of variables is applied to solve a multi-span beam problem, the size of matrix that determines the eigensolutions of the problem increases as the number of subspans increases, which may cause strenuous computations associated with large-order matrices.
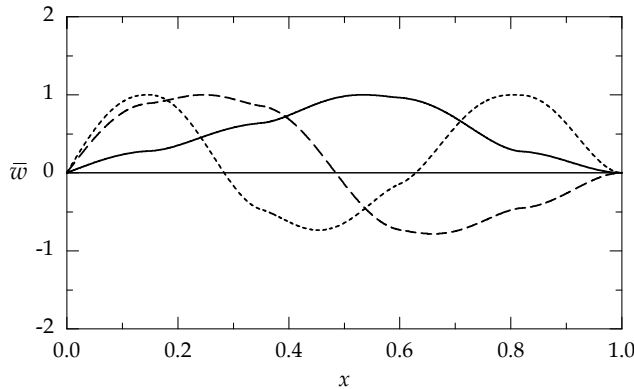

Fig. 8. First three mode shapes obtained from Eq. (3.25). The solid, dashed, and dotted curves represent the 1st , 2nd, and 3rd modes, respectively.

3.4 Transfer function analysis

Consider a multi-span beam subjected to an external force applied at $x=x_0$ where x_0 is located in subspan m. Let $\mathbf{C}^\pm$ be the amplitudes of the waves rise in sub-span n as a result of injected waves due to the applied force, and also assume that $\mathbf{C}^\pm$ satisfy all the continuity conditions at intermediate discontinuities and boundary conditions of the multi-span beam system. The transverse displacement $\bar{w}_n(x;s)$ of span n can be expressed in wave form

$$\bar{w}_n(x;s) = [1 \quad 1][\mathbf{f}(x;s)\mathbf{C}^+ + \mathbf{f}^{-1}(x;s)\mathbf{C}^-] \tag{3.30}$$

Now, in order to determine the actual wave amplitudes $\mathbf{C}^\pm$, consider the multi-span beam with arbitrary supports and boundary conditions under a concentrated applied force of $\bar{p}(s)\delta(x - x_0)$, where $\bar{p}(s)$ is the Laplace transform of $p(\tau)$, as schematically depicted in Fig. 5 with $C_i^\pm$, $D_i^\pm$, and R_i replaced by $\mathbf{C}_i^\pm$, $\mathbf{D}_i^\pm$, and $\mathbf{R}_i$, respectively. Since the waves injected at $x=x_0$ travel in both directions, a new set of local coordinates $\{\xi, \xi\}$ is defined such that the waves traveling towards each end of the beam are measured positive as indicated in the Fig. 5. Let $\mathbf{C}_i^\pm$ and $\mathbf{D}_i^\pm$ be the amplitudes of the waves traveling within subspan i in the region $x<x_0$ and $x \geq x_0$, respectively. The discontinuity in the shear force at $x=x_0$ can be expressed in term of the difference in amplitudes between the incoming and outgoing waves at the discontinuity such that

$$\mathbf{D}_1^+ - \mathbf{C}_1^- = \mathbf{v} \qquad \mathbf{C}_1^+ - \mathbf{D}_1^- = \mathbf{v} \tag{3.31}$$

where $\mathbf{v}$ is the wave vector injected by the applied force which can be determined by the geometric and kinetic continuity conditions at $\xi=0$ as

$$\mathbf{v} = \frac{\overline{p}(s)}{4\gamma^3} \begin{Bmatrix} \sqrt{-1} \\ 1 \end{Bmatrix} \tag{3.32}$$

Applying the global wave reflection matrices on each side of discontinuity 1 gives

$$\mathbf{C}_1^- = \mathbf{R}_{1r}\mathbf{C}_1^+ \quad \mathbf{D}_1^- = \mathbf{R}_{1r}^*\mathbf{D}_1^+ \tag{3.33.1-2}$$

Combining Eqs. (3.31) and (3.33), one can find the wave amplitudes that give rise at the point of loading

$$\mathbf{C}_1^+ = \mathbf{T}_1\mathbf{v} \quad \mathbf{T}_1 = (\mathbf{I} - \mathbf{R}_{1r}^*\mathbf{R}_{1r})^{-1}(\mathbf{I} + \mathbf{R}_{1r}^*) \tag{3.34}$$

$$\mathbf{D}_1^+ = \mathbf{T}_1^*\mathbf{v} \quad \mathbf{T}_1^* = (\mathbf{I} - \mathbf{R}_{1r}\mathbf{R}_{1r}^*)^{-1}(\mathbf{I} + \mathbf{R}_{1r}) \tag{3.35}$$

$\mathbf{T}_1$ and $\mathbf{T}_1^*$ in the above equations can be considered as the generalized wave transmission matrices that characterize the transmissibility of the waves injected by the applied force in the region $x < x_0$ and $x \geq x_0$, respectively. It is evident that $\mathbf{T}_1$ and $\mathbf{T}_1^*$ are different unless the system is symmetric about $x = x_0$. Applying the results in Eqs. (3.34) and (3.35) to Eq. (3.30), the transverse displacement of any point in span 1 on either side of the point of loading can be found. For example, for span 1 in the region $x < x_0$

$$\overline{w}_1(\xi_1, x_0; s) = [1 \quad 1][\mathbf{f}_1(\xi_1; s) + \mathbf{f}_1^{-1}(\xi_1; s)\mathbf{R}_{1r}]\mathbf{T}_1\mathbf{v} \quad 0 \leq \xi_1 \leq l_1 \tag{3.36}$$

In the same manner as for free response analysis, the forced response solution in Eq. (3.36) can be generalized for a multi-span beam by applying the global wave transmission matrix. For $x < x_0$, $\mathbf{C}_1^+ = \mathbf{T}_1\mathbf{v}$ and $\mathbf{C}_{i+1}^+ = \mathbf{T}_i\mathbf{C}_i^+$. Therefore one can progressively expand the solution in Eq. (3.36) until the expansion terminates at the leftmost boundary. Thus, the transverse displacement of any point within span i in the region $x < x_0$ due to external loading at $x = x_0$ can be determined from

$$\overline{w}_i(\xi_i, x_0; s) = \frac{\overline{p}(s)}{4\gamma^3}[1 \quad 1][\mathbf{f}_i(\xi_i; s) + \mathbf{f}_i^{-1}(\xi_i; s)\mathbf{R}_{ir}]\prod_{k=i}^{1}\mathbf{T}_k\begin{Bmatrix} \sqrt{-1} \\ 1 \end{Bmatrix} \quad 0 \leq \xi_i \leq l_i \tag{3.37}$$

One can find the same expression in the region $x \geq x_0$, but in terms of $\mathbf{R}_{ir}^*$ and $\mathbf{T}_k^*$ instead. Note that the ratio $G_i(\xi, x_0; s) = \overline{w}(\xi_i, x_0; s)/\overline{p}(s)$ in Eq. (3.37) is the transfer function governing the forced response of anypoint in span i due to the point loading at $x = x_0$. The Laplace inversion of $G_i(\xi, x_0; s)$ is the Green's function of the problem. Therefore, denoting L^{-1} as the inverse Laplace transform operator, the forced response at any point within any span of the multi-span beam can be found from; e.g., for span i in the region $x < x_0$,

$$w_i(\xi_i, x_0; \tau) = \int_0^t G_i(\xi_i, x_0; \tau - \overline{\tau})p(\tau)d\overline{\tau} \quad (i = 1, 2, \cdots, m) \tag{3.38}$$

$$G_i(\xi_i, x_0; \tau) = L^{-1}\left[\frac{1}{4\gamma^3}[1 \quad 1][\mathbf{f}_i(\xi_i; s) + \mathbf{f}_i^{-1}(\xi_i; s)\mathbf{R}_{ir}]\prod_{k=i}^{1}\mathbf{T}_k\begin{Bmatrix} \sqrt{-1} \\ 1 \end{Bmatrix}\right] \quad 0 \leq \xi_i \leq l_i \tag{3.39}$$

The exact Laplace inversion of $G_i(\xi, x_0; s)$ in close form is prohibitively difficult for the beam problems considered in this study, in particular multi-span beams with non-classical intermediate supports and boundary conditions. One may have to resort to the numerical inversion of Laplace transforms. Shown in Fig. 9 is the unit impuse response curve of a non-uniformly damped three-span beam, whose system parameters are listed in Table 2, sampled at $x=0.15$ and $x=0.825$ for $x_0=0.4$. The unit impulse response curve obtained from the method of normal mode expansion is also shown for comparison. For the results obtained from the method of normal mode expansion, the mode shape function of $\sin n\pi x$ ($n=1, ..., 10$) are used for the expansion and the constraint forces at the intermediate supports are represented by using the Dirac-Delta function. The resulting set of modal equations are numerically integrated using a fixed-step Runge-Kutta algorithm since the beam is nonproportionally damped hence the modal equations cannot be decoupled. It can be seen that both results show an excellent agreement.

			Discontinuity		
Constraint	3	2	1=1*	2	3
Location	0	0.15	0.4	0.65	1
k_t	∞	2,000	0	3,000	∞
k_r	0	0	0	0	0
c_t	0	15	0	10	0

Table 2. Nondimensional system parameter used for Fig. 9, where $c_e=0$.

Regarding the numerical Laplace inversion to obtain the transient response of a Euler-Bernoulli beam model due to an impulse, it should be noted that there exists a singular behavior of the response for small values of time; i.e., the initial response. This is not due to the algorithm of the numerical Laplace inversion, but due to the inherent deficiency of the classical Euler-Bernoulli beam theory that neglects the effects of rotary inertia and shear
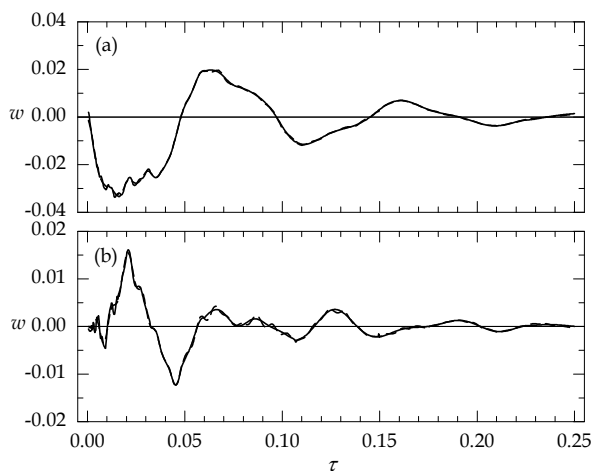

Fig. 9. Unit impulse response of the three-span beam sampled at (a) $x=0.15$ and (b) $x=0.825$. The solid and dashed curves represent the results from the present analysis and the method of normal mode expansion, respectively.

deformations. According to this simple beam theory, a wave of very high frequency (or very short wavelength) would be predicted instantaneously at remote locations, which is physically unacceptable since this can be interpreted as that such a wave travels at an infinity velocity. This abnormal behavior of the Euler-Bernoulli beam can be readily verified by observing the phase velocity c of the dispersion equation (Eq. (3.6) with $s=i\omega$ and $\omega=c\gamma$) continues to increase with increasing γ. Therefore, for a meaningful initial transient response to an impulsive load, one must employ Rayleigh or Timoshenko beam models. Studies on the wave reflection and transmission behavior at various point discontinuities and boundaries using a Timoshenko beam model can be found in Refs. (Tan & Kang, 1999; Mei and Mace, 2005).

If $p(\tau) = p_0 e^{i\omega\tau}$; i.e., a harmonic forcing function, the steady-state response of the problem can be readily found in terms of the complex frequency function defined as

$$H(\xi_i, x_0; \omega) = G(\xi_i, x_0; s)|_{s=i\omega} \qquad (3.40)$$

Constraint	Discontinuity							
	4	3	2	1=1*	2*	3*	4*	5*
Location	0	0.12	0.26	0.39	0.56	0.69	0.84	1
k_t	5,000	4,000	3,500	0	3,000	5,000	∞	0
k_r	100	0	100	0	100	50	0	0
c_t	0.5	0.1	0	0	0	0.1	0.1	0.2

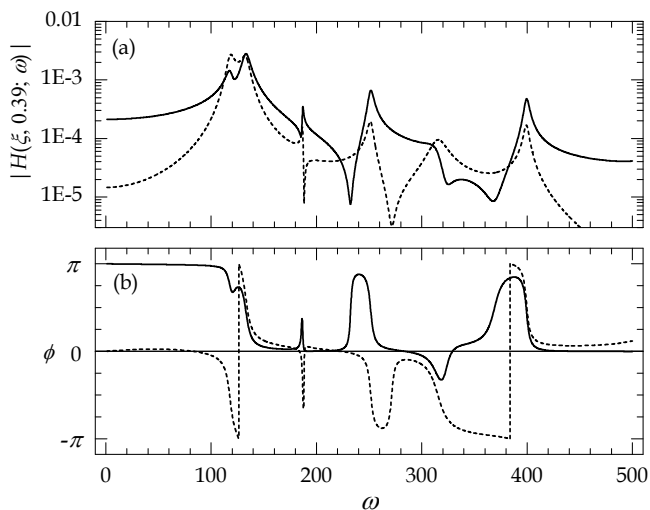Table 3. Nondimensional system parameter used for Fig. 8, where c_e=0.

Fig. 10. Frequency response of the six-span beam due to harmonic excitation applied at x=0.39: (a) amplitudes sampled at x=0.325 (solided curve) and x=0.92 (dashed curve); and (b) corresponding phase angle.

Therefore the frequency response at any point within any subspan of the beam can be obtained by; e.g., for span i in the region $x<x_0$

$$w_i(\xi_i, x_0; \tau) = |H_i(\xi_i, x_0; \omega)| p_0 e^{i(\omega\tau + \phi_i)} \quad 0 \le \xi_i \le l_i \tag{3.41}$$

$$H_i(\xi_i, x_0; \omega) = \frac{1}{4\gamma^3}[1 \quad 1][\mathbf{f}_i(\xi_i; \omega) + \mathbf{f}_i^{-1}(\xi_i; \omega)\mathbf{R}_{ir}] \prod_{k=i}^{1} \mathbf{T}_k \begin{Bmatrix} \sqrt{-1} \\ 1 \end{Bmatrix} \quad \phi_i = \angle H_i \tag{3.42}$$

Shown in Fig.10 is the frequency response sampled at x=0.325 and x=0.92 for the non-uniformly damped six-span beam, whose system parameters are listed in Table 3, under harmonic excitation at x=0.39.

4. Sixth order systems

The analysis techniques described in the previous sections can be applied to the vibrations of higher order, one-dimensional, distributed parameter systems. For example, the in-plane vibration of a planar curved beam is governed by a sixth order partial differential equation. Consider a thin planar curved bam. Neglecting the effects of rotary inertia and shear deformations, the coupled equations of motion governing the flexural displacement W and the tangential displacement U of the centroidal axis are

$$\frac{EI}{R^3}\frac{\partial^3}{\partial\theta^3}\left(U - \frac{\partial W}{\partial\theta}\right) - \frac{EA}{R}\left(W + \frac{\partial U}{\partial\theta}\right) = \rho AR \frac{\partial^2 W}{\partial t^2} \tag{4.1.1}$$

$$\frac{EI}{R^3}\frac{\partial^2}{\partial\theta^2}\left(U - \frac{\partial W}{\partial\theta}\right) + \frac{EA}{R}\frac{\partial}{\partial\theta}\left(W + \frac{\partial U}{\partial\theta}\right) = \rho AR \frac{\partial^2 U}{\partial t^2} \tag{4.1.2}$$

where E denotes the Young's modulus, I the second moment of inertia of the cross-section about the centroid, θ the angular coordinate, R the constant radius of curvature for the given range of angle θ, A the cross-sectional area, ρ the mass density, and t the time variable. Details of deriving these equations of motion can be found in Ref. (Graff, 1975). With the following non-dimensional variables and parameters:

$$u = \frac{U}{R} \quad w = \frac{W}{R} \quad \tau = \frac{t}{t_0} \quad t_0 = R^2\sqrt{\frac{\rho A}{EI}} \quad k^2 = \frac{I}{AR^2} \tag{4.2}$$

where t_0 is a characteristic time constant and k is the curvature parameter, Eq. (4.1) takes the following non-dimensional form in the Laplace domain

$$k^2\frac{\partial^3}{\partial\theta^3}\left(\bar{u}(\theta;s) - \frac{\partial\bar{w}(\theta;s)}{\partial\theta}\right) - \left(\bar{w}(\theta;s) + \frac{\partial u(\theta;s)}{\partial\theta}\right) = k^2 s^2 \bar{w}(\theta;s) \tag{4.3.1}$$

$$k^2\frac{\partial^2}{\partial\theta^2}\left(\bar{u}(\theta;s) - \frac{\partial\bar{w}(\theta;s)}{\partial\theta}\right) + \frac{\partial}{\partial\theta}\left(\bar{w}(\theta;s) + \frac{\partial\bar{u}(\theta;s)}{\partial\theta}\right) = k^2 s^2 \bar{u}(\theta;s) \tag{4.3.2}$$

where s represents the Laplace variable. In order to determine the general wave solutions for the equations of motion in Eq. (4.3), the following form of harmonic wave solutions are first assumed

$$\begin{Bmatrix} \bar{w}(\theta;s) \\ \bar{u}(\theta;s) \end{Bmatrix} = \begin{Bmatrix} C_w \\ C_u \end{Bmatrix} e^{i\gamma\theta} \tag{4.4}$$

where γ denotes the wavenumber, normalized against R, of the wave traveling along the centroidal axis. Substituting the above wave solutions into Eq. (4.3) leads to

$$\begin{bmatrix} k^2(\gamma^4 + s^2) + 1 & i\gamma(1 + \gamma^2 k^2) \\ i\gamma(1 + \gamma^2 k^2) & -k^2(\gamma^2 + s^2) - \gamma^2 \end{bmatrix} \begin{Bmatrix} C_w \\ C_u \end{Bmatrix} = 0 \tag{4.5}$$

Since the determinant of the matrix in Eq. (4.5) must vanish for nontrivial solutions, one can obtain following frequency equation

$$\gamma^6 + (k^2 s^2 - 2)\gamma^4 + [1 + (1 + k^2)s^2]\gamma^2 + (k^2 s^2 + 1)s^2 = 0 \tag{4.6}$$

The six roots (essentially three complex conjugates, namely $\pm\gamma_n(s)$, $n=1$,2, 3) of Eq. (4.6) can be obtained in a closed form by transforming Eq. (4.6) into a cubic equation. Each conjugate pair is the wavenumber of the constituent wave components corresponding to each of the two wave modes of the curved beam. Therefore, it can be found that

$$\bar{w}(\theta; s) = \sum_{n=1}^{3} (C_n^+ e^{-i\gamma_n \theta} + C_n^- e^{i\gamma_n \theta}) \tag{4.7.1}$$

$$\bar{u}(\theta; s) = \sum_{n=1}^{3} \alpha_n (C_n^+ e^{-i\gamma_n \theta} - C_n^- e^{i\gamma_n \theta}) \tag{4.7.1}$$

where the coefficient C represents the amplitude of each flexural wave component with its traveling direction indicated by the $+/-$ signs. The subscript n signifies the spatial wave motion of the same type traveling in the opposite direction. α_n is the amplitude ratio between the flexural and tangential waves which can be found from Eq. (4.5) that

$$\alpha_n = \frac{i\gamma_n(k^2\gamma_n^2 + 1)}{(1 + k^2)\gamma_n^2 + k^2 s^2} \tag{4.8}$$

The above wave solutions may be recast in vector form by grouping the waves traveling in the same direction in a wave packet; i.e., $\mathbf{C}^+ = \{C_1^+ \quad C_2^+ \quad C_3^+\}^T$ and $\mathbf{C}^- = \{C_1^- \quad C_2^- \quad C_3^-\}^T$, then

$$\bar{w}(\theta; s) = \mathbf{u}[\mathbf{f}\mathbf{C}^+ + \mathbf{f}^{-1}\mathbf{C}^-] \tag{4.9.1}$$

$$\bar{u}(\theta; s) = \boldsymbol{\alpha}[\mathbf{f}\mathbf{C}^+ - \mathbf{f}^{-1}\mathbf{C}^-] \tag{4.9.2}$$

where $u = [1 \quad 1 \quad 1]$, $\boldsymbol{\alpha} = [\alpha_1 \quad \alpha_2 \quad \alpha_3]$, and $\mathbf{f}$ is the field transfer matrix defined by

$$\mathbf{f}(\theta; s) = \begin{bmatrix} e^{-i\gamma_1 \theta} & 0 & 0 \\ 0 & e^{-i\gamma_2 \theta} & 0 \\ 0 & 0 & e^{-i\gamma_3 \theta} \end{bmatrix} \tag{4.10}$$

One now can see that the analysis techniques described in the previous sections for the multi-span beam can be applied to a multi-span curved beam in the same manner to

determine the local wave reflection and transmission matrices, global wave reflection and transmission matrices, and the transfer function (Kang et al., 2003). The only difference is the size of matrix, three by three for the curved beam. It should be also noted that the present analysis techniques are applicable to one-dimensional distributed parameter systems involving other types of discontinuities such as geometric/material changes and cracks, as long as the properties of those discontinuities can be characterized by wave reflection and transmission coefficients or matrices. In what follows, an example of free vibration analysis of a three-span curved beam with curvature changes is presented.

4.1 Wave reflection and transmission at a curvature change

Consider a curved beam with two subspans of different curvatures joined at $\xi=0$. Assuming that the wavenumbers of the waves traveling in each subspan are γ_n and γ_n' ($n=1, 2, 3$), the geometric continuity conditions at $\xi=0$ give

$$
\begin{bmatrix}
1 & 1 & 1 \\
\alpha_1 & \alpha_2 & \alpha_3 \\
\alpha_1 - i\gamma_1 & \alpha_2 - i\gamma_2 & \alpha_3 - i\gamma_3
\end{bmatrix} \mathbf{C}^+ +
\begin{bmatrix}
1 & 1 & 1 \\
-\alpha_1 & -\alpha_2 & -\alpha_3 \\
-\alpha_1 + i\gamma_1 & -\alpha_2 + i\gamma_2 & -\alpha_3 + i\gamma_3
\end{bmatrix} \mathbf{r}\mathbf{C}^+
$$
$$
=
\begin{bmatrix}
1 & 1 & 1 \\
\alpha_1' & \alpha_2' & \alpha_3' \\
\alpha_1' - i\gamma_1' & \alpha_2' - i\gamma_2' & \alpha_3' - i\gamma_3'
\end{bmatrix} \mathbf{t}\mathbf{C}^+
\tag{4.11.1}
$$

and the kinetic continuity conditions give

$$
\begin{bmatrix}
1 - i\gamma_1\alpha_1 & 1 - i\gamma_2\alpha_2 & 1 - i\gamma_3\alpha_3 \\
-\gamma_1^2(i\gamma_1 + \alpha_1) & -\gamma_2^2(i\gamma_2 + \alpha_2) & -\gamma_3^2(i\gamma_3 + \alpha_3) \\
\gamma_1(\gamma_1 - i\alpha_1) & \gamma_2(\gamma_2 - i\alpha_2) & \gamma_3(\gamma_3 - i\alpha_3)
\end{bmatrix} \mathbf{C}^+
$$
$$
+
\begin{bmatrix}
1 - i\gamma_1\alpha_1 & 1 - i\gamma_2\alpha_2 & 1 - i\gamma_3\alpha_3 \\
\gamma_1^2(i\gamma_1 + \alpha_1) & \gamma_2^2(i\gamma_2 + \alpha_2) & \gamma_3^2(i\gamma_3 + \alpha_3) \\
\gamma_1(\gamma_1 - i\alpha_1) & \gamma_2(\gamma_2 - i\alpha_2) & \gamma_3(\gamma_3 - i\alpha_3)
\end{bmatrix} \mathbf{r}\mathbf{C}^+
\tag{4.11.2}
$$
$$
=
\begin{bmatrix}
1 - i\gamma_1'\alpha_1' & 1 - i\gamma_2'\alpha_2' & 1 - i\gamma_3'\alpha_3' \\
-\gamma_1'^2(i\gamma_1' + \alpha_1') & -\gamma_2'^2(i\gamma_2' + \alpha_2') & -\gamma_3'^2(i\gamma_3' + \alpha_3') \\
\gamma_1'(\gamma_1' - i\alpha_1') & \gamma_2'(\gamma_2' - i\alpha_2') & \gamma_3'(\gamma_3' - i\alpha_3')
\end{bmatrix} \mathbf{t}\mathbf{C}^+
$$

$$
\alpha_n' = \frac{i\gamma_n'(k'^2\gamma_n'^2 + 1)}{(1 + k'^2)\gamma_n'^2 + k'^2 s^2}
\tag{4.11.3}
$$

The local wave reflection and transmission matrices can be found by solving the above equations. The curved beam system shown in Fig. 11 has three subspans of equal span angle of 60° but different radius of curvature. Both ends are clamped. The natural frequencies of the system can be obtained from

$$
F(s) = \text{Det}[\mathbf{r}_1 \mathbf{R}_{1r} - \mathbf{I}_{3\times3}] = 0
\tag{4.12}
$$

where $\mathbf{r}_1$ is the wave reflection matrix at the clamed boundary, which is

$$\mathbf{r}_1 = \begin{bmatrix} -1 & -1 & -1 \\ -\alpha_1 & -\alpha_2 & -\alpha_3 \\ \alpha_1 - i\gamma_1 & \alpha_2 - i\gamma_2 & \alpha_3 - i\gamma_3 \end{bmatrix}^{-1} \begin{bmatrix} -1 & -1 & -1 \\ -\alpha_1 & -\alpha_2 & -\alpha_3 \\ \alpha_1 - i\gamma_1 & \alpha_2 - i\gamma_2 & \alpha_3 - i\gamma_3 \end{bmatrix} \qquad (4.13)$$

and $\mathbf{R}_{1r}$ is the global wave reflection matrix that includes the effects of the curvature changes and the other clamped boundary. The natural frequencies are compared in Table 4 with the results obtained by the finite element method (FEM) (Maurizi et al., 1993; Krishnan and Suresh, 1998) and the cell discretization method (CDM) (Maurizi et al., 1993). Note that the natural frequencies obtained from the present wave analysis are exact since both propagating and attenuating wave components are considered in the formulation.
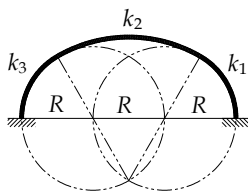
Fig. 11. Curved beam with three subspan of equal span angle of 60°, where $k_1=k_3=0.01$ and $k_2=0.02$.

	Present	FEM		CDM
		12 curved elements	24 straight elements	100 Degrees of freedom
Mode		Ref. 1	Ref. 2	Ref. 1	Ref. 1
1	2.683	2.680	2.701	2.685	2.671
2	4.834	4.824	4.828	4.828	4.780
3	9.565	9.536	9.543	9.543	9.413
4	14.585	14.527	14.535	14.535	14.309
5	21.865	21.749	21.751	21.751	21.265

Table 4. Non-dimensional natural frequencies of the curved beam in Fig. 11.

5. Summary

An alternative approach to the dynamic response analysis of one-dimensional distributed parameter systems by applying the concepts of wave motions in elastic waveguides is presented. The analysis techniques are demonstrated using the vibration of multi-span strings, straight beams, and curved beams with general support and boundary conditions, however other one-dimensional systems such as rods and higher order beam models can be treated in the same manner. The present approach allows a systematic formulation that leads to exact, closed-form, distributed transfer functions from which the transient response and frequency response solutions can be obtained. In addition, the present analysis approach results in recursive computational algorithms that always involve computations of fixed-size matrices regardless of the number of subspans, which can be implemented into highly efficient computer codes. Since neither exact nor approximate eigensolutions are required as a priori, the present wave-based approach is suitable for the forced response analysis of non-self-adjoint systems. There are two limiting cases that may affact the analysis accuracy and

numerical efficiency of the present wave approach: (1) when the waveguide contains a *very* small amount of inertia or flexibilty (such as massless elements or rigid bodies), which results in making the wavelenght of the constituent waves larger than the span length of the waveguide; and (2) when the waveguide is extremely flexible or its response contains a very sharp impulsive spike (such as the impulse response example shown in Section 2.4), which result in making the wavelength of the constituent waves unrealistically small. In paractice, however, most engineering structures have resonable amounts of inertia, flxibility, and also damping such that these two limiting cases will be rarely encountered.

6. References

Abate, J. & Valkó, P. P. (2004). Multi-Precision Laplace Transform Inversion, *International Journal of Numerical Methods in Engineering*, Vol.60, pp.979-993

Argento, A. & Scott, R. A. (1995). Elastic Wave Propagation in a Timoshenko Beam Spinning about Its Logitudinal Axis, *Wave Motion,* Vol.21, pp. 67-74

Cremer, L.; Heckl, M. & Ungar, E. E. (1973). *Structure-Borne Sound,* Springer, Berlin, Germany

Fahy, F. (1987). *Sound and Structural Vibration*, Academic Press, Orlando, USA

Graff, K. F. (1975). *Wave Motion in Elastic Solids*, Ohio State University Press, Columbus, Ohio, USA

Kang, B. & Tan, C. A. (1998). Elastic Wave Motions in an Axially Strained, Infinitely Long Rotating Timoshenko Shaft, *Journal of Sound and Vibration*, Vol.213, No.3, pp.467-482

Kang, B. (2007). Transfer Functions of One-Dimensional Distributed Parameter Systems by Wave Approach, *ASME Journal of Vibration and Acoustics*, Vol. 129, pp.193-201

Kang, B.; Riedel, R. H. & Tan, C. A. (2003). Free Vibration Analysis of Planar Curved Beams by Wave Propagation, *Journal of Sound and Vibration*, Vol.260, pp.19-44

Krishnan, A. & Suresh, Y. J. (1998) A Simple Cubic Linear Elements for Static and Free Vibration Analyses of Curved Beams, *Computer and Structures*, Vol.68, pp.473-489

Mace, B. R. (1984). Wave Reflection and Transmission in Beams, *Journal of Sound and Vibration*, Vol.97, No.2, pp.237-246

Maurizi, M. J.; Belles, R. E. & Rossi, M. A. (1993). Free Vibration of a Three-Centered Arc Clamped at the Ends, *Journal of Sound and Vibration*, Vol.213, pp.483-510

Mead, D. J. (1994). Wave and Modes in Finite Beams: Application of the Phase-Closure Principle, *Journal of Sound and Vibration*, Vol.171, pp.695-702

Mei, C. & Mace, B. R. (2005). Wave Reflection and Transmission in Timoshenko Beams and Wave Analysis of Timoshenko Beam Structures, *ASME Journal of Vibration and Acoustics*, Vol.127, pp.382-394

Tan, C. A. & Kang, B. (1999). Wave Reflection and Transmission in an Axially Strained, Rotating Timoshenko Shaft, *Journal of Sound and Vibration*, Vol.213, pp.483-510

Yang, B. & Tan, C. A. (1992). Transfer Functions of One-Dimensional Distributed Parameter Systems, *ASME Journal of Applied Mechanics*, Vol. 58, pp.1009-1014

Yang, B. (1996). Closed-Form Transient Response of Distributed Damped Systems, Part I: Modal Analysis and Green's Function Formula, *ASME Journal of Applied Mechanics*, Vol. 63, pp.997-1003

Yang, B. (1996). Closed-Form Transient Response of Distributed Damped Systems, Part II: Energy Formulation fo Constrained and Combined Systems, *ASME Journal of Applied Mechanics*, Vol. 63, pp.1004-1010

Yong, Y. & Lin, Y. K. (1989). Propagation of Decaying Waves in Periodic and Pieccewise Periodic Structures of Finite Length, *Journal of Sound and Vibration*, Vol.129, pp.99-118
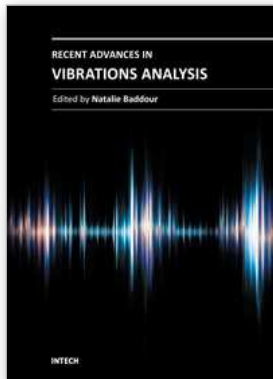
Recent Advances in Vibrations Analysis

Edited by Dr. Natalie Baddour

This book covers recent advances in modern vibrations analysis, from analytical methods to applications of vibrations analysis to condition monitoring. Covered topics include stochastic finite element approaches, wave theories for distributed parameter systems, second other shear deformation theory and applications of phase space to the identifications of nonlinearities and transients. Chapters on novel condition monitoring approaches for reducers, transformers and low earth orbit satellites are included. Additionally, the book includes chapters on modelling and analysis of various complex mechanical systems such as eccentric building systems and the structural modelling of large container ships.

How to reference

In order to correctly reference this scholarly work, feel free to copy and paste the following:

Bongsu Kang (2011). Exact Transfer Function Analysis of Distributed Parameter Systems by Wave Propagation Techniques, Recent Advances in Vibrations Analysis, Dr. Natalie Baddour (Ed.), ISBN: 978-953-307-696-6, InTech, Available from: http://www.intechopen.com/books/recent-advances-in-vibrations-analysis/exact-transfer-function-analysis-of-distributed-parameter-systems-by-wave-propagation-techniques

INTECH
open science | open minds